Research in Astron. Astrophys. **2011** Vol. **11** No. **8**, 902–908
http://www.raa-journal.org *http://www.iop.org/journals/raa*

Research in Astronomy and Astrophysics

External photon fields in Fermi bright blazars *

Xiao-Yan Gao[1,2,3], Jian-Cheng Wang[1,2] and Ming Zhou[1,2,3]

[1] National Astronomical Observatories / Yunnan Observatories, Chinese Academy of Sciences, Kunming 650011, China; *xy-gao@ynao.ac.cn*
[2] Key Laboratory for the Structure and Evolution of Celestial Objects, Chinese Academy of Sciences, Kunming 650011, China
[3] Graduate University of Chinese Academy of Sciences, Beijing 100049, China

Received 2011 January 28; accepted 2011 April 7

Abstract The external Compton (EC) model is used to study the high energy emission of some blazars, in which the external photon field is considered to dominate inverse Compton radiation. We explore the properties of the external photon field through analyzing the *FERMI* LAT bright AGN sample within three months of the start of operations in sky-survey mode. In the sample, assuming the high energy radiation of low synchrotron peaked blazars is from the EC process, we find that the external photon parameter $U_{\rm ext}/\nu_{\rm ext}$ may not be a constant. Calculating synchrotron and inverse Compton luminosity from the quasi-simultaneous broadband spectral energy distributions, we find that they have an approximately linear relation. This indicates that the ratio of external photon and magnetic energy density is a constant in the comoving frame, implying that the Lorentz factor of the emitting blob depends on the external photon field and magnetic field. The result gives a strong constraint on the dynamic jet model.

Key words: galaxies: active — galaxies: jets — gamma-rays: galaxies —- radiation mechanism: non-thermal

1 INTRODUCTION

Blazars, presenting weak (or even absent) broad emission lines and large optical polarizations, are a radio loud subclass of active galactic nuclei (AGNs). They are thought to be objects emitting non-thermal radiation across the entire electromagnetic spectrum from a relativistic jet which is closely aligned along the line of sight and hence appears Doppler boosted (Begelman & Rees 1984; Urry 1999). The broadband spectral energy distribution (SED) of blazars is double humped with a first peak usually in the soft-to-medium X-ray range and a second one in the GeV–TeV energy band (Sambruna et al. 1996). The first peak is generally dominated by synchrotron emission (Marscher & Gear 1985) but the second one is uncertain.

The high energy emission is usually attributed to Compton upscattering of soft photons. The soft photons may come from a synchrotron process called the synchrotron self Compton (SSC) model (Maraschi et al. 1992; Marscher & Gear 1985), or from a process with external field photons which is

* Supported by the National Natural Science Foundation of China.

called the External Compton (EC) model. The external field photons can possibly include accretion disk radiation (e.g., Dermer et al. 1992; Dermer & Schlickeiser 1993), broad line region (BLR) (Sikora et al. 1994; Blandford & Levinson 1995; Ghisellini & Madau 1996; Dermer et al. 1997), dust torus (Błażejowski et al. 2000) or synchrotron emission from other regions (Georganopoulos & Kazanas 2003; Ghisellini & Tavecchio 2008). All these different scenarios have been tested by specific sources.

Blazars contains BL Lac objects and flat spectrum radio quasars (FSRQs). In previous literatures, BL Lac objects are often subdivided into two or three subclasses depending on their SED which was first introduced by Padovani & Giommi (1995). Depending on the peak energy of the synchrotron emission, BL Lacs are classified into low-frequency or high-frequency BL Lac objects, called LBL and HBL respectively. Abdo et al. (2010) give a new classification to all types of non-thermal dominated AGNs. They are low synchrotron peaked (LSP), intermediate synchrotron peaked (ISP) and high synchrotron peaked (HSP) blazars, defined by the location of the low energy SED peak. The LSP sources, consisting of flat spectrum radio quasars and low frequency peaked BL Lac objects (LBLs), have the synchrotron peak in the far-infrared or infrared regime with $\nu_{\rm peak}^{\rm S}\leq 10^{14}$ Hz. The ISP sources, mainly including LBLs and intermediate BL Lac objects (IBLs), have their synchrotron peak in optical-UV frequencies with $10^{14}\leq\nu_{\rm peak}^{\rm S}\leq 10^{15}$ Hz, while the HSP objects, almost all known to be high-frequency-peaked BL Lac objects (HBLs), have their synchrotron peak at X-ray energies with $\nu_{\rm peak}^{\rm S}> 10^{15}$ Hz.

In the framework of leptonic models, the blazar sequence FSRQ→ LBL → IBL→ HBL is thought to be a decreasing contribution of external radiation fields to radiative cooling of electrons and production of high energy radiation (Ghisellini et al. 1998; Celotti & Ghisellini 2008). The $\gamma-$ray radiation of FSRQs is always thought to be attributed to the EC model (Cao & Bai 2008; Liu et al. 2008). In this paper, we use the sample of LSP blazars from the first three months of observations from the *Fermi Gamma Ray Space Telescope* to study the properties of high energy emission and an external photon field based on the EC model. The peak frequencies and fluxes are obtained through fitting the SEDs which are quasi-simultaneous multifrequency measurements instead of using an empirical method from spectral slopes $\alpha_{\rm ox}$ and $\alpha_{\rm ro}$. We find that the external photon parameter in the observer frame $U_{\rm ext}/\nu_{\rm ext}$ is not constant. We also find that there is a linear correlation between synchrotron luminosity $L_{\rm S}$ and inverse Compton (IC) luminosity $L_{\rm IC}$, implying that the ratio between the external radiation and the magnetic field energy densities inside the source (in the comoving frame) depends on the Lorentz factor. In Section 2 we present the sample of LSP sources. In Section 3 we show the statistical method and results. The discussion and results are shown in Section 4.

We adopt a concordance cosmology with $H_0=70\,{\rm km\,s^{-1}\,Mpc^{-1}}$, $\Omega_\Lambda=0.7$ and $\Omega_{\rm M}=0.3$.

2 THE SAMPLE

The Large Area Telescope (LAT) onboard the *Fermi Gamma Ray Space Telescope*, launched on 2008 June 11, provides unprecedented sensitivity in the $\gamma-$ray band (20 MeV to over 300 GeV, Atwood et al. 2009). The first three months of operations in the sky-survey mode, from 2008 August 4 to October 31, led to the compilation of a list of 106 high confidence $\gamma-$ray sources. Abdo et al. (2010) give the quasi-simultaneous SEDs of 48 blazars from the LAT observation. They include 23 FSRQs, 19 BL Lacs and one unknown type of blazar, all of which have known redshifts.

The sample we adopted consists of 30 low synchrotron peak (LSP) blazars, including 23 FSRQs and seven low energy peak BL Lacs. In view of the blazar sequence, the gamma-ray emission of these LSPs could be dominated by external Compton radiation. We also present eight high energy peak BL Lacs for contrast. Usually, the HBLs lack an emission line, and the SSC radiation could dominate their gamma-rays. All sources are listed in Table 1. Column 1 gives the source name presented by

Abdo et al. (2009); Column 2 gives the redshift; Columns 3, 4, 5 and 6 are the peak frequencies and fluxes of synchrotron and inverse Compton (IC) emission. We use the peak frequencies $\nu^{\rm S}_{\rm peak}$ and $\nu^{\rm EC}_{\rm peak}$ and the peak fluxes $\nu^{\rm S}_{\rm peak}F(\nu^{\rm S}_{\rm peak})$ and $\nu^{\rm EC}_{\rm peak}F(\nu^{\rm EC}_{\rm peak})$, given by Abdo et al. (2010) who used a simple third-degree polynomial to fit the SED (Kubo et al. 1998), where the data are from quasi-simultaneous multifrequency observations. Column 7 lists the total synchrotron luminosity; Column 8 is the total IC luminosity; Column 9 is the IC luminosity calculated by the EC model; and Column 10 gives the classifications.

3 MODEL AND TEST

We consider the homogeneous EC model to study the properties of a high energy SED for LSP sources. The synchrotron and IC peak frequencies are given by Tavecchio et al. (1998)

$$\nu^{\rm S}_{\rm peak} = \frac{4}{3}\nu_{\rm L}\gamma_{\rm b}^2\delta, \tag{1}$$

and

$$\nu^{\rm EC}_{\rm peak} = \frac{4}{3}\nu_{\rm ext}\gamma_{\rm b}^2\Gamma\delta, \tag{2}$$

where $\nu_{\rm L} = eB/(2\pi m_{\rm e}c)$ is the Larmor frequency, $\gamma_{\rm b}$ is the Lorentz factor of electron spectral break and $\nu_{\rm ext}$ is the concentrated frequency of external photons. Here, Γ is the Lorentz factor of the emitting blob. While δ is the Doppler factor defined by $\delta = 1/(1 - v/c\cos\theta)$, v is the relativistic bulk velocity and θ is the angle of the jet relative to the observer's line of sight.

The ratio between the total luminosity of synchrotron and IC radiation is related to the ratio between the external field and magnetic energy density, given as

$$\frac{L_{\rm IC}}{L_{\rm S}} = \frac{U^{'}_{\rm ext}}{U^{'}_{\rm B}} \simeq \frac{17}{12}\frac{\Gamma^2 U_{\rm ext}}{U^{'}_{\rm B}}, \tag{3}$$

where $U^{'}_{\rm ext} \simeq (17/12)\Gamma^2 U_{\rm ext}$ is the external photon energy density in the comoving frame (Ghisellini & Madau 1996) and $U^{'}_{\rm B}$ is the magnetic field energy density inside the source (in the comoving frame). Here we declare that parameters with prime notation " ′ " represent the approaching frame, otherwise they are in the observer frame.

From the above equations we obtain

$$\frac{L_{\rm IC}}{L_{\rm S}} \simeq \frac{17e^2}{6\pi m_{\rm e}^2 c^2}\frac{U_{\rm ext}}{\nu^2_{\rm ext}}\left(\frac{\nu^{\rm EC}_{\rm peak}}{\nu^{\rm S}_{\rm peak}}\right)^2 . \tag{4}$$

The SEDs of the sources in the sample are fitted by Abdo et al. (2010). We use the SEDs to obtain the differential luminosity of synchrotron and IC radiation. We then calculate the total luminosity $L_{\rm S}$ and $L_{\rm IC}$ by integrating the differential luminosity. The results are shown in Columns 7 and 8 of Table 1. Assuming $L_{\rm IC}$ mainly comes from external Compton emission, we examine the relation of $L_{\rm IC}/L_{\rm S}$ and $\nu^{\rm EC}_{\rm peak}/\nu^{\rm S}_{\rm peak}$ shown in Figure 1 and find that the relation is rather disperse. No obvious correlation implies that the parameter $U_{\rm ext}/\nu^2_{\rm ext}$ of the external photons is not a constant in Equation (4). The result is different from the common scenario of the external photon from the BLR (Ghisellini et al. 1998; Celotti & Ghisellini 2008; Ghisellini & Madau 1996; Tavecchio & Ghisellini 2008). In particular, we take the common values of $U_{\rm BLR} = 2.65 \times 10^{-2}$ erg cm^{-3} and $\nu_{\rm ext}$=2 $\times$ $10^{15}\Gamma$ Hz and calculate the EC luminosity $L_{\rm EC}$ from $L_{\rm S}$ using Equation (4) shown in Column 9. We find that the $L_{\rm EC}$ of many sources is larger than the $L_{\rm IC}$ from the SEDs, indicating that the previous results on the external photon field have questionable validity.

Table 1 List of Sources and Basic Parameters Studied in This Paper

Name 0FGL (1)	z (2)	$\log \nu^{\rm S}_{\rm peak}$ [Hz] (3)	$\log(\nu F\nu)^{\rm S}_{\rm peak}$ [erg cm^{-2} s^{-1}] (4)	$\log \nu^{\rm IC}_{\rm peak}$ [Hz] (5)	$\log(\nu F\nu)^{\rm IC}_{\rm paek}$ [erg cm^{-2} s^{-1}] (6)	$\log L_{\rm S}$ [erg s^{-1}] (7)	$\log L_{\rm IC}$ [erg s^{-1}] (8)	$\log L_{\rm EC}$ [erg s^{-1}] (9)	Class (10)
J0137.1+4751	0.859	13.6	–10.8	22.6	–10.6	47.03	46.70	47.29	FSRQ
J0210.8−5100	1.003	12.5	–10.5	22.4	–10.2	47.06	47.73	49.13	FSRQ
J0229.5−3640	2.115	13.5	–10.7	21.8	–10.4	46.73	47.95	45.59	FSRQ
J0238.4+2855	1.213	12.8	–11.7	22.1	–10.8	46.92	47.57	47.79	FSRQ
J0238.6+1636	0.94	13.5	–10.0	23.2	–9.90	47.07	47.50	48.73	BL Lac
J0349.8−2102	2.944	12.9	–10.7	21.8	–10.2	47.35	48.34	47.42	FSRQ
J0423.1−0112	0.916	13.4	–11.3	21.7	–10.3	46.34	47.91	45.20	FSRQ
J0428.7−3755	1.03	13.3	–11.0	22.8	–10.2	46.54	48.14	47.81	BL Lac
J0457.1−2325	1.003	13.1	–10.9	22.8	–9.90	46.88	47.89	48.55	FSRQ
J0531.0+1331	2.07	12.8	–11.0	21.3	–9.80	47.06	48.98	46.33	FSRQ
J0538.8−4403	0.892	13.4	–10.6	22.7	–10.1	47.05	47.22	47.92	BL Lac
J0730.4−1142	1.598	13.1	–11.1	22.6	–10.0	46.98	48.17	48.25	FSRQ
J0855.4+2009	0.306	13.4	–9.8	21.4	–10.5	46.71	46.18	44.97	BL Lac
J0921.2+4437	2.19	13.4	–10.9	22.0	–10.6	47.55	47.73	47.02	FSRQ
J1159.2+2912	0.729	13.1	–11.2	22.0	–10.5	46.58	46.60	46.65	FSRQ
J1229.1+0202	0.158	13.5	–10.7	21.0	–9.60	46.55	46.33	43.82	FSRQ
J1256.1−0548	0.536	12.6	–9.8	22.2	–10.3	45.84	45.74	47.31	FSRQ
J1310.6+3220	0.997	13.1	–10.3	22.5	–10.4	46.99	47.68	48.06	FSRQ
J1457.6−3538	1.424	13.6	–10.9	22.7	–10.2	47.23	48.44	47.69	FSRQ
J1504.4+1030	1.839	13.6	–11.7	22.9	–9.80	45.89	46.70	46.56	FSRQ
J1512.7−0905	0.36	13.1	–10.9	22.3	–9.70	46.56	48.21	47.02	FSRQ
J1522.2+3143	1.487	13.3	–10.6	22.4	–10.2	46.45	47.28	46.71	FSRQ
J1719.3+1746	0.137	13.5	–10.3	24.7	–10.7	44.69	45.84	49.36	BL Lac
J1751.5+0935	0.322	13.1	–10.8	22.2	–10.3	45.95	46.14	46.42	BL Lac
J1849.4+6706	0.657	13.5	–10.6	22.5	–10.5	45.91	45.96	43.98	FSRQ
J2143.2+1741	0.213	14.1	–10.4	22.0	–10.5	47.74	48.23	47.81	FSRQ
J2202.4+4217	0.069	13.6	–10.1	21.9	–10.8	45.28	44.85	44.14	BL Lac
J2254.0+1609	0.859	13.6	–11.5	22.5	–9.80	45.55	46.25	46.21	FSRQ
J2327.3+0947	1.843	13.1	–11.0	21.5	–10.3	47.59	48.24	48.46	FSRQ
J2345.5−1559	0.621	13.3	–9.5	22.5	–10.7	46.85	48.49	45.91	FSRQ
J0033.6−1921	0.61	16.1	–11.1	24.3	–11.1	46.23	46.17	44.90	BL Lac
J0449.7−4348	0.205	15.6	–10.2	23.9	–10.5	46.29	46.17	44.15	BL Lac
J0507.9+6739	0.416	16.6	–10.7	24.3	–10.5	46.35	46.32	44.01	BL Lac
J1015.2+4927	0.2	16.3	–10.5	24.5	–10.6	45.78	46.15	44.44	BL Lac
J1104.5+3811	0.03	16.6	–9.4	25	–9.9	45.16	44.62	44.23	BL Lac
J1653.9+3946	0.033	17.1	–10.3	24.7	–10.5	45.25	44.07	42.71	BL Lac
J2000.2+6506	0.047	16.6	–10	24.7	–10.5	44.57	44.56	43.03	BL Lac
J2158.8−3014	0.116	16	–9.7	23.9	–10.2	46.22	46.00	44.28	BL Lac

Notes: Columns (1) source LAT names; (2) redshift; (3) synchrotron peak frequency; (4) synchrotron peak flux; (5) IC peak frequency; (6) IC peak flux; (7) synchrotron luminosity; (8) IC luminosity; (9) IC luminosity calculated by the EC model and (10) classification.

We also show the relation between $L_{\rm IC}$ and $L_{\rm S}$ in Figure 2, indicating a significant correlation. The best fit to the $L_{\rm IC}$–$L_{\rm S}$ relationship is

$$\log L_{\rm IC} = 1.1 \log L_{\rm S} - 4.5 \quad (5)$$

with a correlation coefficient $R = 0.58$ and the relationship is nearly linear, spanning a wide range of both luminosities. The relation indicates that $L_{\rm IC}/L_{\rm S}$ is approximately constant, implying the ratio

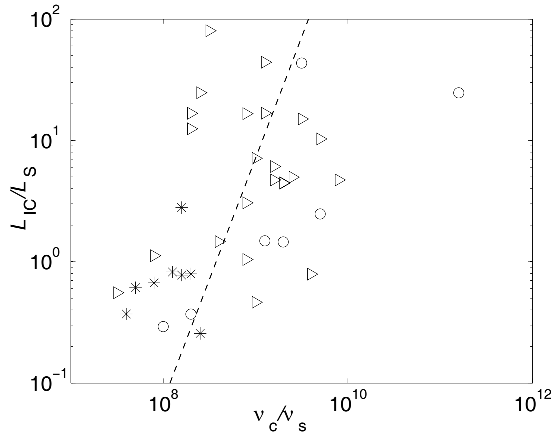

Fig. 1 Relation between $L_{\rm IC}/L_{\rm S}$ and $\nu_{\rm peak}^{\rm EC}/\nu_{\rm peak}^{\rm S}$. *Triangles*: FSRQs (LSPs), *circles*: BL Lac objects (LSPs) and *asterisks*: BL Lacs which are HSPs. *Dashed line* is the fitted line with a slope of 2.

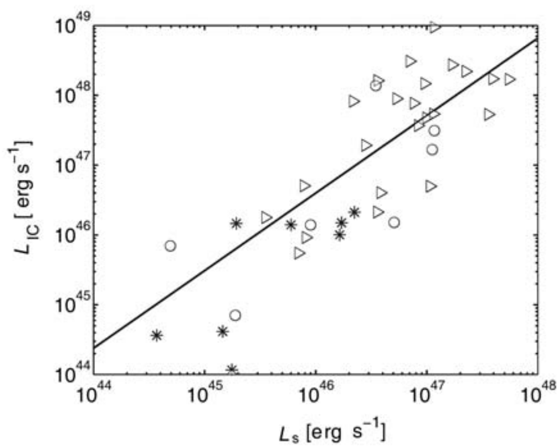

Fig. 2 Relation between the total luminosity $L_{\rm S}$ and $L_{\rm IC}$. Symbols are the same as in Fig. 1.

of external photon and magnetic energy density is constant in the comoving frame. If the gamma-ray blob is inside the BRL, from Equation (3), we will obtain $\Gamma \propto (U_{\rm B}^{'}/U_{\rm ext}^{'})^{1/2}$, implying that the motion of the jet could be related to the magnetic field and external photon. Usually, the magnetic field assumes an important role in the acceleration and collimation of the relativistic jet (Leismann et al. 2005; McKinney 2006; Keppens et al. 2008), while the external photons can affect the jet dynamics through radiative drag (Sikora et al. 1996; Luo & Protheroe 1999). Therefore, the relation we obtained provides observational evidence for the balance between the acceleration and deceleration of the jet. The main contribution for high energy radiation of HSPs is always considered to be the SSC emission and the EC emission could supplement high energy radiation. For comparison, we plot HSPs in Figure 2 and find that HSPs behave similarly with LSPs, located in the low luminosity range.

4 CONCLUSIONS AND DISCUSSION

The BL Lac objects in our sample include two subsamples: LBLs and HBLs. The LBLs together with FSRQs are considered as LSPs (Abdo et al. 2010) as mentioned above. External Compton scattering is likely to be the main emission process responsible for the copious amounts of γ-rays produced in LSP blazars. The soft seed photons outside the γ-ray emitting region dominate the gamma-ray emission. Usually, the HBLs lack a broad emission line, so the SSC could dominate their gamma-rays. Equation (3) is obviously invalid for the HBLs, but the HSPs in Figure 1 only show their position for comparison with other sources and do not represent their relations to gamma-ray emission mechanisms. For LBLs, if the gamma-rays originate from the blob inside the BLR and the size of the BLR is proportional to $L^{0.5}$ (Celotti & Ghisellini 2008), the energy density and peak frequency of external photons will be constant to a good approximation. It is indicated that the ratio between EC and synchrotron luminosity just depends on the peak frequency $(\nu^{\rm S}_{\rm peak}/\nu^{\rm EC}_{\rm peak})^2$. In the paper we have presented, the statistical analysis of a sample of 30 LSP blazars from the *Fermi*-LAT observation is presented. After examining the relation between $L_{\rm IC}/L_{\rm S}$ and $\nu^{\rm EC}_{\rm peak}/\nu^{\rm S}_{\rm peak}$for LSP blazars, we find there is almost no correlation between them, which means that the parameter $U_{\rm ext}/\nu^2_{\rm ext}$ of the external photons is not constant or Equation (3) is invalid for some LSPs due to the gamma-ray blob being located outside the BLR. Our statistical results show that the gamma-rays of LSPs could be produced in different external photon fields. There are two kinds of emissive scenarios. (1) The gamma-ray blob is inside the BLR, so Figure 1 implies that the external photons could come from many components including the BLR and do not have constant energy density (Bai et al. 2009; Cao & Bai 2008). (2) The gamma-ray blob is outside the BLR, so the external photons from the BLR are Doppler deboosted for the blob. The relation given by Equation (4) is invalid, leading to no correlation between $L_{\rm IC}/L_{\rm S}$ and $\nu^{\rm EC}_{\rm peak}/\nu^{\rm S}_{\rm peak}$, shown in Figure 1. We also consider the relation of $L_{\rm IC}$ and $L_{\rm S}$ and find an approximately linear relationship between them, although the statistical significance is not high due to the lack of a large sample. This result shows that the ratio of external field to magnetic energy density in the emitting blob is approximately constant. This implies that the Lorentz factor depends on the external photon field and magnetic field when the blob is inside the BLR. The result indicates evidence of balancing the jet motion under the action of radiative drag and influences from the magnetic field, which can be used to constrain the jet dynamic model.

Acknowledgements We acknowledge financial support from the National Natural Science Foundation of China (Grant No. 10778702), the National Basic Research Program of China (Grant No. 2009CB824800) and the Policy Research Program of Chinese Academy of Sciences (KJCX2-YW-T24).

References

Abdo, A. A., Ackermann, M., Agudo, I., et al. 2010, ApJ, 716, 30
Abdo, A. A., Ackermann, M., Ajello, M., et al. 2009, ApJS, 183, 46
Atwood, W. B., Abdo, A. A., Ackermann, M., et al. 2009, ApJ, 697, 1071
Bai, J. M., Liu, H. T., & Ma, L. 2009, ApJ, 699, 2002
Begelman, M. C., & Rees, M. J. 1984, MNRAS, 206, 209
Blandford, R. D., & Levinson, A. 1995, ApJ, 441, 79
Błażejowski, M., Sikora, M., Moderski, R., & Madejski, G. M. 2000, ApJ, 545, 107
Cao, X., & Bai, J. M. 2008, ApJ, 673, L131
Celotti, A., & Ghisellini, G. 2008, MNRAS, 385, 283
Dermer, C. D., & Schlickeiser, R. 1993, ApJ, 416, 458
Dermer, C. D., Schlickeiser, R., & Mastichiadis, A. 1992, A&A, 256, L27

Dermer, C. D., Sturner, S. J., & Schlickeiser, R. 1997, ApJS, 109, 103
Georganopoulos, M., & Kazanas, D. 2003, ApJ, 594, L27
Ghisellini, G., Celotti, A., Fossati, G., Maraschi, L., & Comastri, A. 1998, MNRAS, 301, 451
Ghisellini, G., & Madau, P. 1996, MNRAS, 280, 67
Ghisellini, G., & Tavecchio, F. 2008, MNRAS, 386, L28
Keppens, R., Meliani, Z., van der Holst, B., & Casse, F. 2008, A&A, 486, 663
Kubo, H., Takahashi, T., Madejski, G., et al. 1998, ApJ, 504, 693
Leismann, T., Antón, L., Aloy, M. A., et al. 2005, A&A, 436, 503
Liu, H. T., Bai, J. M., & Ma, L. 2008, ApJ, 688, 148
Luo, Q., & Protheroe, R. J. 1999, MNRAS, 304, 800
Maraschi, L., Ghisellini, G., & Celotti, A. 1992, ApJ, 397, L5
Marscher, A. P., & Gear, W. K. 1985, ApJ, 298, 114
McKinney, J. C. 2006, MNRAS, 368, 1561
Padovani, P., & Giommi, P. 1995, ApJ, 444, 567
Sambruna, R. M., Maraschi, L., & Urry, C. M. 1996, ApJ, 463, 444
Sikora, M., Begelman, M. C., & Rees, M. J. 1994, ApJ, 421, 153
Sikora, M., Sol, H., Begelman, M. C., & Madejski, G. M. 1996, MNRAS, 280, 781
Tavecchio, F., & Ghisellini, G. 2008, MNRAS, 386, 945
Tavecchio, F., Maraschi, L., & Ghisellini, G. 1998, ApJ, 509, 608
Urry, C. M. 1999, Astroparticle Physics, 11, 159